ACS Chemical Neuroscience

Research Article

Cite This: ACS Chem. Neurosci. 2019, 10, 2730−2740

pubs.acs.org/chemneuro

Prolines Affect the Nucleation Phase of Amyloid Fibrillation Reaction; Mutational Analysis of Human Stefin B

Samra Hasanbašić,[†,‡] Ajda Taler-Verčič,[§,∥] Vida Puizdar,[§] Veronika Stoka,[†,§] Magda Tušek Žnidarič,[⊥] Andrej Vilfan,[#] Selma Berbić,[‡] and Eva Žerovnik*[,†,§,∥]

[†]Jožef Stefan International Postgraduate School, Jamova 39, 1000 Ljubljana, Slovenia

[‡]Faculty of Pharmacy, Department of Biochemistry, University of Tuzla, Univerzitetska 1, 75000 Tuzla, Bosnia and Herzegovina

[§]Department of Biochemistry and Molecular and Structural Biology and [#]Department of Condensed Matter Physics, Jožef Stefan Institute, Jamova 39, 1000 Ljubljana, Slovenia

[∥]Center of Excellence for Integrated Approaches in Chemistry and Biology of Proteins, Jamova 39, 1000 Ljubljana, Slovenia

[⊥]Department of Biotechnology and Systems Biology, National Institute of Biology, Večna pot 111, 1000 Ljubljana, Slovenia

Supporting Information

ABSTRACT: Proline residues play a prominent role in protein folding and aggregation. We investigated the influence of single prolines and their combination on oligomerization and the amyloid fibrillation reaction of human stefin B (stB). The proline mutants influenced the distribution of oligomers between monomers, dimers, and tetramers as shown by the size-exclusion chromatography. Only P74S showed higher oligomers, reminiscent of the molten globule reported previously for the P74S of stB-Y31 variant. The proline mutants also inhibited to various degree the amyloid fibrillation reaction. At 30 and 37 °C, inhibition was complete for the P74S single mutant, two double mutants (P6L P74S and P74S P79S), and for the triple mutant P6L P11S P74S. At 30 °C the single mutant P6L completely inhibited the reaction, while P11S and P79S formed amyloid fibrils with a prolonged lag phase. P36D did not show a lag phase, reminiscent of a downhill polymerization model. At 37 °C in addition to P36D, P11S, and P79S, P6L and P11S P74S also started to fibrillate; however, the yield of the fibrils was much lower than that of the wild-type protein as judged by transmission electron microscopy. Thus, Pro 74 *cis/trans* isomerization proves to be the key event, acting as a switch toward an amyloid transition. Using our previous model of nucleation and growth, we simulated the kinetics of all the mutants that exhibited sigmoidal fibrillation curves. To our surprise, the nucleation phase was most affected by Pro *cis/trans* isomerism, rather than the fibril elongation phase.

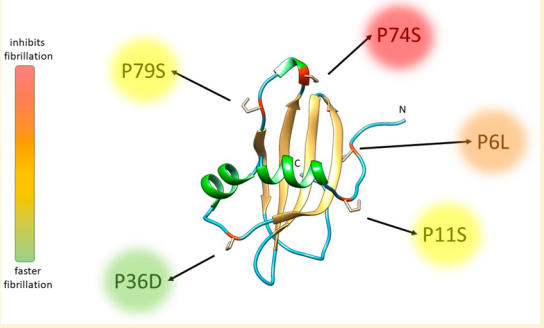

KEYWORDS: *Amyloid fibrils, cystatins, conformational disease, domain-swapped dimer, protein aggregation, protein folding, proteinopathies, the kinetics of amyloid fibril formation, proline mutants, proline switch*

INTRODUCTION

The primary aim of studying the mechanism of ordered aggregation of proteins into amyloid fibrils is to gain insight into the basic molecular processes underlying proteinopathies, also called conformational diseases.[1] Neurodegenerative diseases, such as Alzheimer's disease, Parkinson's disease, prion-associated encephalopathies,[2] ataxias, amyotrophic lateral sclerosis, etc.,[3,4] all share the features of protein mis-folding, aggregation, and amyloid fibril formation.

Amyloid fibril formation is proposed to be a process that is common to both pathogenic and nonpathogenic proteins.[5] Currently no unifying mechanism has been accepted; in contrast, the aggregation regimes can change from downhill polymerization to nucleated polymerization with an extensive lag phase, depending on the interplay of inherent protein properties (sequence, post-translational modifications) and solution conditions. An initial partial unfolding or folding of intrinsically disordered proteins (IDPs) is followed by further conformational changes, which lead to a greater β-sheet structure content. Nucleation is a common feature of the proposed mechanisms, where the necessary conformational changes are facilitated in the oligomeric nucleus.

Cells have developed several protective mechanisms to counteract protein aggregation.[4,6] Apart from the chaperone machinery and two degradation systems, these inherent protective mechanisms include phosphorylation, acetylation, and the inherent properties of the amino acid sequence. The molecular switches include conserved proline (Pro) residues, which not only modulate the rates of folding[7−9] but also affect both oligomerization and amyloid fibril formation.[10,11] A growing body of evidence suggests that certain Pro residues increase the fibrillation propensity due to the process of *cis/*

Received: November 12, 2018
Accepted: March 29, 2019
Published: March 29, 2019

DOI: 10.1021/acschemneuro.8b00621
ACS Chem. Neurosci. 2019, 10, 2730−2740

Table 1. Characteristics of stefin B wt and Its Pro Mutants

protein	oligomeric state	typical fibrillation pattern at 30 °C	typical fibrillation pattern at 37 °C
stB wt (C3S)	monomers and dimers	Forms classical fibrils after initial lag phase ~60 h	Forms classical fibrils after initial lag phase ~20 h
P6L	as stB wt	Did not fibrillate *under observed period of time*	*Prolonged lag phase*
P11S	as stB wt	Prolonged the lag phase	Prolonged the lag phase
P36D	as stB wt	*Shortened the lag phase*	*Shortened the lag phase*
P74S	molten globule	Did not fibrillate under observed period of time	Did not fibrillate under observed period of time
P79S	monomers, dimers, and tetramers	*Prolonged the lag phase*	*Prolonged the lag phase*
***P6L* P74S**	monomers, dimers, and open monomer	Did not fibrillate under observed period of time	Did not fibrillate under observed period of time
P11S **P74S**	dimers, monomers, and open monomer	Did not fibrillate *under observed period of time*	*Prolonged the lag phase*
P74S P79S	monomers, dimers (equal ratio), and open monomer	Did not fibrillate under observed period of time	Did not fibrillate under observed period of time
P6L P11S **P74S**	monomer and open monomer	Did not fibrillate under observed period of time	Did not fibrillate under observed period of time

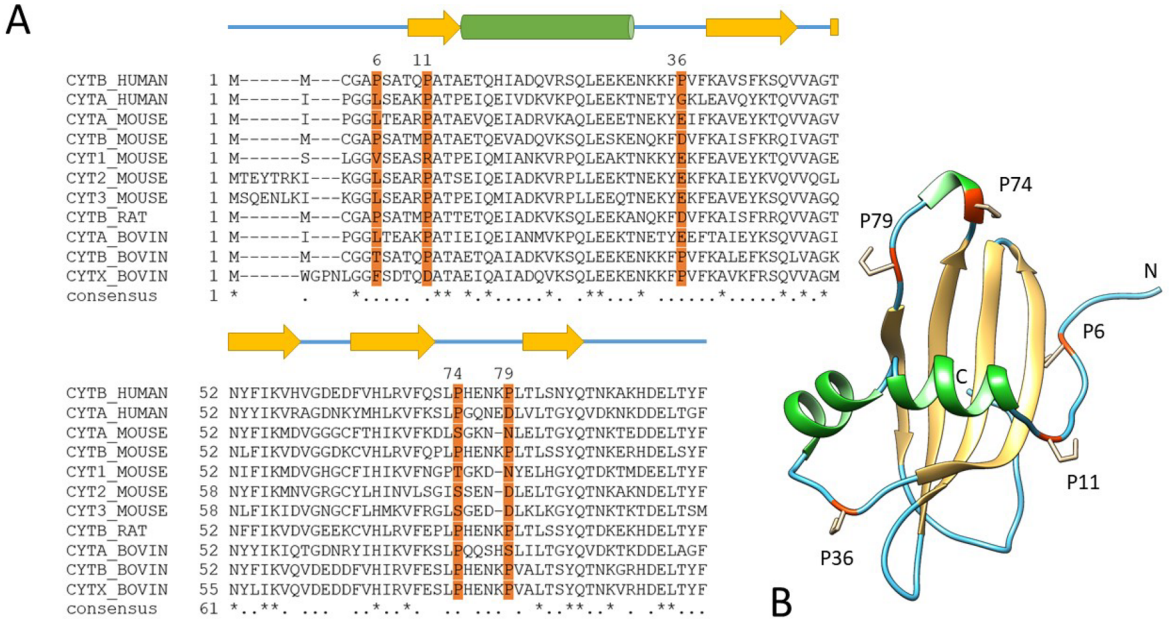

Figure 1. (A) Sequence alignment of stefin B and its homologues from different organisms. Human stefin B sequence (UniProt P04080) is compared with human stefin A (UniProt P01040), mouse cystatin A (UniProt P56567), mouse cystatin B (UniProt Q62426), mouse stefin 1 (UniProt P35175), mouse stefin 2 (UniProt P35174), mouse stefin 3 (UniProt P35173), rat cystatin B (UniProt P01041), bovine cystatin A (UniProt P80416), bovine cystatin B (UniProt P25417) and bovine cystatin C (UniProt P35478). Proline residues are marked in orange; numbering is according to human stefin B sequence. Multiple sequence alignment was performed using T-Coffee server.[1] Secondary structure elements are schematically shown above the sequence alignment. beta-strands are in yellow and α-helix is in green. (B) Three-dimensional ribbon representation of human stefin B structure (pdb id: 1STF). Secondary structure elements are colored the same way as in schematic representation (see A). Prolines are marked in orange and presented as sticks. N- and C-terminus are labeled by letters. Credit: Reproduced with permission from Notredame, C., Higgins, D.G., and Heringa, J. T-Coffee: A novel method for fast and accurate multiple sequence alignment. *J. Mol. Biol.* 302, 205-217. Copyright 2000 Academic Press.

trans isomerization of the peptide bond preceding Pro. Prolines participate in domain swapping, as they control the rigidity of loops between secondary structure elements.[12,13] It is known that peptide bonds mostly appear in the *trans* conformation in both the folded and unfolded states of proteins, because *trans* is the energetically favored state. The *cis/trans* isomerization involves rotation around a partial double bond, which makes it an intrinsically costly and slow reaction. Peptide bonds preceding Pro, and sometimes other amino acids in a strained *cis* conformation, can be structurally important and can slow protein folding.[14]

Prolyl isomerases, for example, cyclophilins, provide a powerful tool for studying prolyl isomerization.[15] They catalyze *cis/trans* Pro isomerization, and if acceleration of a folding reaction occurs in the presence of a cyclophilin the folding is related to Pro isomerization. Pro-limited folding reactions can be investigated using site-directed mutagenesis.[16] In this case changes in folding kinetics can be related to Pro residues only if a *cis* prolyl bond is substituted with a *trans* nonprolyl bond, which ultimately leads to an increase of the fast refolding amplitude and the disappearance of slow, Pro-limited reaction.[14] The stefin B fibrillation reaction is proline isomerization-dependent, which was shown by the addition of the peptidyl prolyl *cis/trans* isomerase, CypA. CypA prolongs the lag phase and increases the fibril yield. Addition of an inactive CypA, which has a disabling mutation in the active

DOI: 10.1021/acschemneuro.8b00621
ACS Chem. Neurosci. 2019, 10, 2730−2740

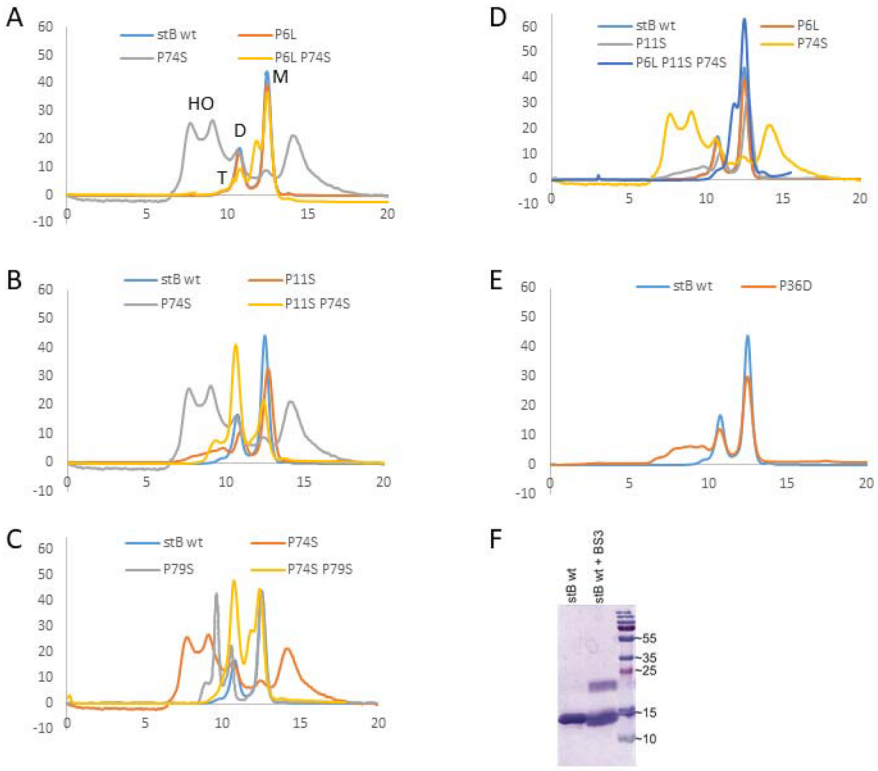

Figure 2. Oligomeric state of human stefin B and its single, double, and triple mutants studied by SEC-FPLC on Superdex 75. (A) elution profiles of stB wt, P6L, P74S, and P6L P74S. (B) Elution profiles of stB wt, P11S, P74S, and P11S P74S; (C) elution profiles of stB wt, P74S, P79S, and P74S P79S; (D) elution profiles of stB wt, P6L, P11S, P74S, and P6L P11S P74S; (E) elution profiles of stB wt and P36D. stB wt was used as a standard. SEC was performed in 10 mM phosphate buffer with 0.15 M NaCl, pH 7.5 at room temperature. Protein concentration was 1 mg/mL. M, D, T, and HO stand for monomers, dimers, tetramers, and higher oligomers. (F) SDS-PAGE electrophoresis of stB wt after cross-linking with BS.[3]

site, also prolongs the lag phase but does not affect the final fibril yield.[17]

The protein inhibitors, cystatins, are the main regulators of lysosomal cysteine cathepsins and other papain-like enzymes. Their main function is to protect the organism against harmful proteolytic activity when cathepsins are released from lysosomes and to serve as a defense mechanism against proteases of invading pathogens.[18] Cystatins are competitive, reversible, and rather nonspecific tight-binding inhibitors of cysteine proteases.[19] On the basis of their amino acid sequences and tertiary structure, the cystatin family is divided into three subfamilies: stefins (I25A), cystatins (I25B), and kininogens (I25C), according to MEROPS database (http://merops.sanger.ac.uk). Stefins are single-chain proteins of ∼100 amino acid residues, lacking disulfide bonds and carbohydrates. The first two structurally homologous members of the stefin family, stefin A and stefin B, were isolated and characterized from human and other mammals.[19] Stefin B is more widely distributed than stefin A and is found in various cells and tissues. Both inhibitors rapidly and tightly inhibit papain-like endopeptidases, such as bovine cathepsins B, L, and S[20] and protozoal enzymes including Cruzipain from *T. cruzi*.[21] The crystal structure of the human stefin B-papain complex shows that stefin B forms a "wedge-shaped edge", which is highly complementary to the active site of the papain.[22] The interacting parts of stefin B consist of the N-terminal region and two hairpin loops composed of a highly conserved region, containing residues Q53 to G57 (QVVAG) and residues P74−H75.

Human stefin B (stB) is of interest as a model protein, as it contains five Pro residues at positions 6, 11, 36, 74, and 79.[8] This has provided a framework for studying folding[23,24] and amyloid fibrillation.[8,25−30] Our in vitro studies have revealed several slow phases in stB folding.[31,32] Furthermore, we have shown that stB readily fibrillates under mildly acidic conditions.[28] Pro residues at positions 74 and 79 have been shown to be responsible for slow folding phases and facilitate domain swapping and loop swapping.[33,34] Mutation of Pro 74 to Ser in the stB-Y31 variant (in which residue E31 is mutated to Y) led to an oligomeric molten globule state,[35] whereas the P36G mutation of the same variant decreased protein stability.[23] When Pro 79 was mutated into a Ser in stB-Y31, the protein oligomerized predominantly as a tetramer.[33] In accordance, in our folding studies of the stB-Y31 variant, we observed a slow folding phase with an amplitude of ∼30%, which correlated with dimerization.[31,32]

Similar cases showing the importance of Pro *cis*/*trans* isomerism in fibrillation have been reported in other proteins, for example, in β_2-microglobulin (β2m), a protein related to dialysis-related amyloidosis (DRA). The His 31−Pro 32 bond in β2m has an unfavorable *cis* conformation, with *cis* to *trans* isomerism of Pro 32 leading directly to amyloid fibril formation.[36] To our knowledge, no systematic analysis of proline mutagenesis and its influence on fibrillation has been reported. Therefore, we systematically mutated the Pro residues of human stefin B to understand their influence in both oligomer and amyloid fibril formation (Table 1).

DOI: 10.1021/acschemneuro.8b00621
ACS Chem. Neurosci. 2019, 10, 2730−2740

2. RESULTS AND DISCUSSION

2.1. Secondary Structure and Oligomeric State of the Mutants. Amino acid substitutions of Pro residues in recombinant human stB wild-type (stB wt) were chosen by comparison with the sequences of other stefins (Figure 1A). Hence, Pro 6 was substituted with Leu (L), Pro 36 was substituted with Asp (D), and Pro 11, Pro 74, and Pro 79 were substituted with Ser (S). We created a set of single, double, and triple Pro mutants, and their calculated properties are summarized in Supporting Information: Table S1.

The purity and inhibitory activity of the isolated proteins were checked (Supporting Information Figures S1 and S2). To evaluate the effects of Pro mutations on stB secondary structure, CD spectra were recorded in the far-UV region (Supporting Information: Figure S3). Negative bands at 208 and 222 nm provide information about the α-helical structure of proteins, which can be explained by n $\rightarrow$ π^* transition for the peptide bond of α-helix in this area.[37] A negative peak at 217 nm reflects β-sheet structure. The CD spectra of stB wt and its Pro mutants are typical of a mostly β-sheet containing protein, whereas the differences in overall intensity and intensity of the peak at 225 nm might arise from different distributions of oligomers.

The stability of Pro mutants was analyzed using NanoDSF (Supporting Information: Figure S4). Most of the Pro mutations increased the overall stability, with the exceptions of P36D and P11S, which were less stable (Figure S4). We observed before that the P36G of stB−Y31 variant was also less stable than the stB-Y31 protein itself and that it was prone to form amorphous aggregates.[23] In this study, the strongest stabilizing effect was observed for P79S and P6L, and all the multiple mutants with this change. Previously, we established that P74S[17] was more stable than stB wt, even though it is prone to transforming into molten globular oligomers (as described below).

Figure 2A−E presents the equilibrium oligomeric state of StB wt and each Pro mutant under nonamyloidogenic conditions at pH 7.5, as determined using size exclusion chromatography (SEC). The oligomeric state of stB wt was also confirmed with sodium dodecyl sulfate−polyacrylamide gel electrophoresis (SDS-PAGE) after cross-linking (Figure 2F). The integration of SEC peaks is given in Supporting Information: Table S2. Elution profiles of P6L (Figure 2A), P11S (Figure 2B), and P36D (Figure 2E) do not differ significantly from stB wt, which elutes as a mixture of monomers and dimers (Figure 2A−E). P79S elutes as a mixture of monomers, dimers, and tetramers (Figure 2C), whereas the P79S mutation of stB-Y31 variant eluted predominantly as a tetramer.[33] P74S (Figure 2A−D) elutes as a broad peak with a large percentage of higher oligomers, which, together with CD spectra, suggest a molten globule state. The P74S mutant of stB-Y31 variant was also found to be molten globular and oligomeric.[33] There are some inconsistencies with our previous results.[8,17,33] These are likely to be caused by different freeze−thaw cycles, which can affect the oligomerization profile of the sensitive P74S mutant.[25]

The double mutant P6L P74S elutes predominantly as monomers with a low content of dimers, whereas P11S P74S elutes predominantly as dimers with fewer monomers (Figure 2A,B). This is an interesting observation, because the oligomeric profiles of both single mutants P6L and P11S are similar to that of stB wt. It appears that mutation of Pro 6 and Pro 74 stabilizes the monomeric form, which has a substantial impact on the fibrillation kinetics of the double mutant P6L P74S (Figure 3). The double mutant P74S P79S forms both

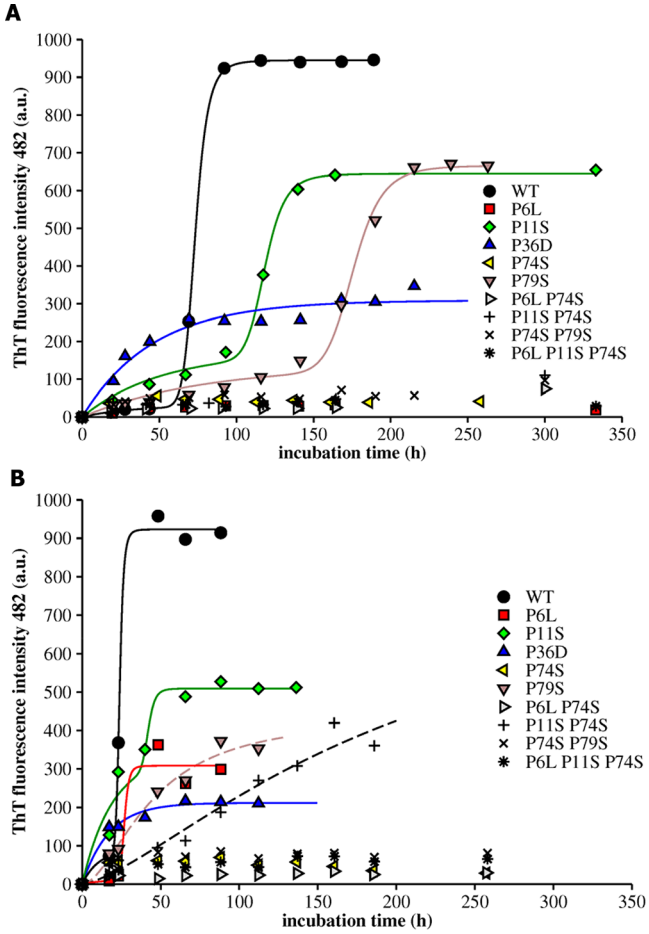

Figure 3. Amyloid fibrillation kinetics of stB wt and its Pro mutants. Time course of ThT dye binding/fluorescence for recombinant human stefin B and its single, double, and triple Pro mutants at (A) 30 and (B) 37 °C. Fibrils were grown under mild conditions (0.015 M acetate buffer, pH 4.8, 0.15 M NaCl) at 30 and 37 °C; protein concentrations were 34 μM. To accelerate fibril formation, fibrillation mixtures contained 10% (v/v) TFE. ThT stock solution was 15 μM, dissolved in a phosphate buffer pH 7.5 as described in section 2. Experiments were conducted three times, each time in two parallels. The curves were obtained by applying equations for mathematical simulation of the reaction as given before.[1] The dotted curves were fitted as explained under Methods.

monomers and dimers to similar extents but not tetramers (Figure 2C), which were observed in the single mutant P79S. Again, it seems that the presence of Pro 74 causes a shift of the equilibrium toward lower oligomers, that is, monomers and dimers, with an impact on the fibrillation kinetics of the double mutant P74S P79S (Figure 3). These observations can be rationalized with changes in the rigidity of the loop, as mutations of both Pro 74 and Pro 79 reside in the same loop. Interestingly, the triple mutant P6L P11S P74S elutes predominantly as a monomer (Figure 2D), similar to P6L P74S, and this again reflects a lowering of fibrillation propensity (Figure 3). This suggests that both P6 and P74 mutations lead synergistically to monomer stabilization. It appears that stabilizing the closed monomer prevents fibril

DOI: 10.1021/acschemneuro.8b00621
ACS Chem. Neurosci. 2019, 10, 2730−2740

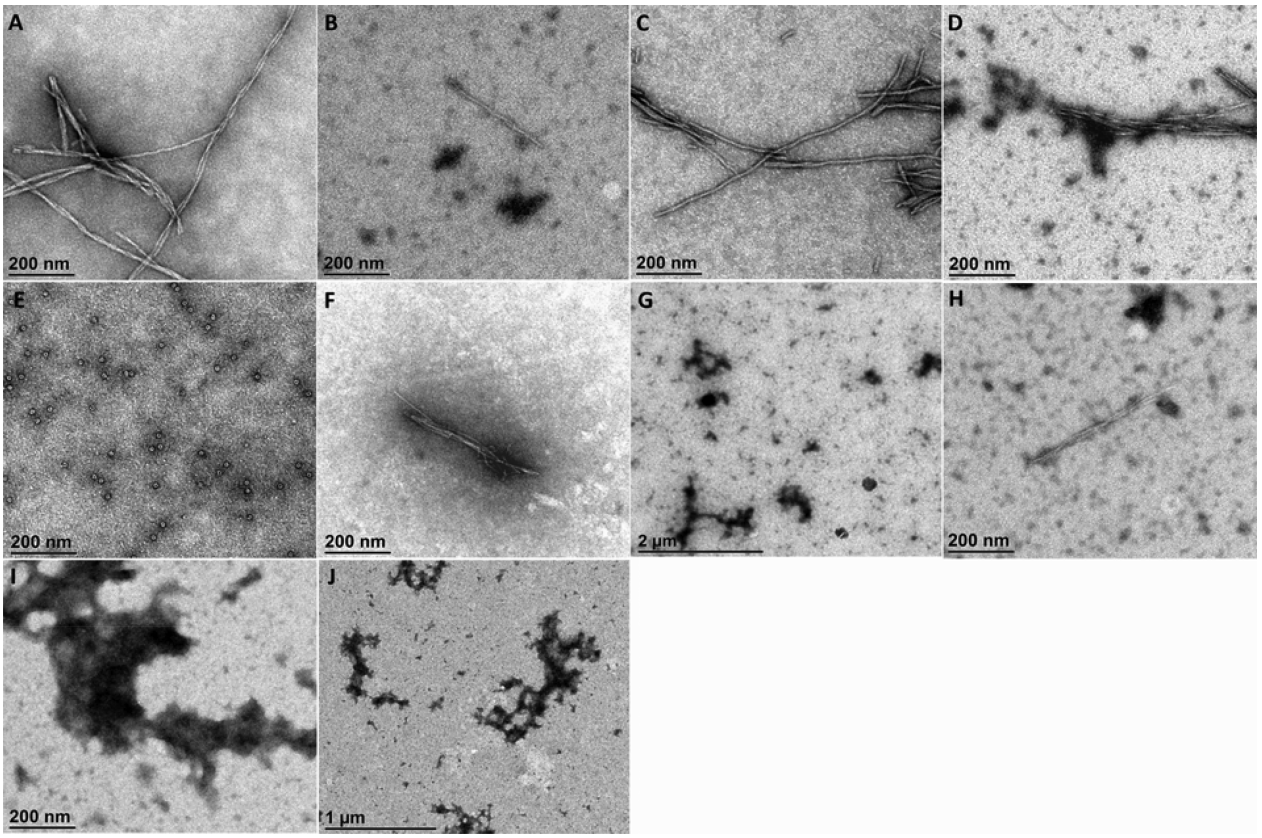

Figure 4. TEM images of the amyloid fibrils and the aggregates formed by stB wt and its Pro mutants. (A) stB wt; (B) mutant P6L; (C) mutant P11S; (D) mutant P36D; (E) mutant P74S; (F) mutant P79S; (G) mutant P6L P74S; (H) mutant P11S P74S; (I) mutant P74S P79S; (J) mutant P6L P11S P74S. Protein concentration was 34 μM. Samples were incubated at 30 °C. Aliquots for TEM analysis were taken at the *plateau* phase of amyloid fibrillation. All micrographs are taken at the same magnification, except micrographs G and J. Each experiment wasperformed once; however, two parallels were observed. The images are most representative.

growth, supporting earlier findings that lower oligomers, starting with open monomers and domain-swapped dimers, initiate amyloid fibrillation of stB wt.[25]

The oligomeric profiles of all double and one triple Pro mutants display an additional peak between monomers and dimers at ∼12 mL. This form has already been detected in equilibrium with dimers.[25] On the one hand, considering that domain-swapped dimers are building blocks of fibrils[34] and that monomers must partially open to initiate domain swapping, this intermediate form has been designated to be an *open monomer*.[25,33,38] On the other hand, stB forms four different types of dimers due to *cis/trans* Pro isomerization.[25,33] Therefore, the additional peak at ∼12 mL might also be caused by elution of a more elongated domain-swapped dimer.

Importantly, the initial oligomeric state is correlated with the observed fibrillation kinetics (section 2.2), where increased monomer stability appears to prevent formation of the oligomeric nucleus.

2.2. Kinetics of Amyloid Fibril Formation and Morphology at the Plateau. There are indications that stefin B amyloid fibrils elongate through domain-swapped dimer addition and conversion.[34] The fibril formation process follows a typical sigmoidal curve; the process starts with a lag phase, where the number of amyloid fibrils is not significant enough to be detected. This is followed by a steep growth phase, where the fibril concentration increases rapidly and eventually reaches the *plateau* phase, where most of the soluble protein has turned into fibrils.[1]

The fibrillation kinetics were followed using Thioflavin T (ThT) fluorescence[39] monitoring at 482 nm (Figure 3). Almost all reactions showed a prolonged lag phase followed by a steep fibril growth phase. The single mutant P36D was an exception; a distinct lag phase was not observed, and in a few hours the whole reaction reached the *plateau* phase at both 30 and 37 °C. The abrupt protofibril formation is in our opinion due to the position of P36 and was also observed for P36G of the stB-Y31 variant.[23] P36 is an α-helix breaker, and replacing it with another amino acid residue may lead to a non-native intermediate with an extended α-helix, which may be precursor to protofibrils. Indeed, the final yield of the fibrils by P36D was lower in comparison to that of stB wt, and the fibrils were shorter, more like protofibrils (as detected by TEM—Figure 4D). Two single mutants, namely, P11S and P79S, showed a prolonged lag phase and lower final fluorescence intensity at both 30 and 37 °C (Figure 3A,B). P6L did not form amyloid fibrils at 30 °C in the observed time period (Figure 3A). At 37 °C it prolonged the lag phase followed by steep fibril growth (Figure 3B). P74S did not fibrillate at all in the observed time period (Figure 3A,B), whereas the previous study of this mutant has shown a 10× longer lag phase at 25 °C.[17] According to TEM analysis (as shown below), this mutant formed annular structures (Figure 4E). Similarly, double and triple mutants did not form amyloid fibrils at 30 °C in the observed time period (Figure 3A). However, at 37 °C the double mutant P11S P74S started to fibrillate with a prolonged lag phase (Figure 3B). The two double mutants P6L P74S and

DOI: 10.1021/acschemneuro.8b00621
ACS Chem. Neurosci. 2019, 10, 2730−2740

P74S P79S and the triple mutant P6L P11S P74S, also did not form fibrils either at 30 or 37 °C in the observed time period (Figure 3B).

The essential role of Pro 74 for amyloid fibril growth has been shown previously.[17] Pro 74 was found in the non-native *cis* conformation in the crystal structure of stB tetramer (P79S stefinB-Y31[33]), and *trans/cis* isomerization of this Pro slows the formation of domain-swapped dimers and/or tetramers. From the present data we can conclude that several proline residues influence the amyloid fibril formation of stB. If they are substituted, amyloid fibril formation is slowed or inhibited through the slowing of nucleation (Figure 3 and Table 2). The propensity to inhibit the reaction toward amyloid fibrils follows this order: P74S = P6L ≫ P79S > P11S at 30 °C and P74S ≫ P6L > P79S > P11S at 37 °C. Thus, Pro 74 remains the key residue, acting as a switch toward the amyloid transition, while Pro 6 is the second most important. It is of interest that these key residues coincide with the protease interacting sites, which consist of the N-terminal region (containing G4 and P6) and two hairpin loops, one containing Q53 to G57 (QVVAG) and the second containing P74 and P79.

Table 2. Consensus Prediction of Aggregation-Prone Regions for Human stB and Its Proline Mutants[a]

protein	AMYLPRED2 Consensus hits
stB	47−58, 64−72
P6L	47−58, 64−72
P11S	47−58, 64−72
P36D	37−39, 47−58, 64−72
P74S	47−58, 64−72
P79S	47−58, 64−72, 81−84
P6L P74S	47−58, 64−72
P11S P74S	47−58, 64−72
P74S P79S	47−58, 64−72, 81−84
P6L P11S P74S	47−58, 64−72

[a]The aggregation-prone regions were retrieved by consensus prediction (CONSENSUS5) using AMYLPRED2 (Tsolis et al., 2013). The consensus hits are indicated by residue number on the stB sequence, namely, V37FK39, V47VAGTNYFIKVH58, F64VHLRVFQS72, and T81LSN84.

2.3. Transmission Electron Microscopy (TEM). ThT fluorescence normally correlates with the amount of amyloid fibrils, and new assays to trace protein aggregation in cells are being explored.[40] Here we used TEM to determine the morphology of the prevailing structures and correlated this with the ThT measurements. Samples for TEM analysis were taken during the *plateau* phase of the reaction at 30 °C (Figure 4). TEM images of stB wt fibrils were taken as a positive control.

It can be seen that stB wt forms typical amyloid fibrils (Figure 4A). Similarly, in the case of P11S (Figure 4C) only fibrils were observed. P36D forms shorter fibrils, the final yield was lower in comparison to stB wt (Figure 4D), and aggregates were always present. In a previous study of P36G stB-Y31 the formation of amorphous aggregate was also suggested.[23] P74S forms annular aggregates (Figure 4E), in accordance with a previous study of P74S stB-Y31, where the aggregates were established to be molten globular and toxic.[35] In case of P79S similar fibrils to those of stB wt were observed, with some aggregates present (Figure 4F). Two double mutants, that is, P6L P74S and P74S P79S, and the triple mutant did not form fibrils under chosen conditions, and only aggregates were observed (Figure 4G,I,J). P11S P74S and P6L predominantly form aggregates, and only a few fibrils can be detected (Figure 4H,B), which is consistent with the observed lower ThT final yield.

2.4. Comparing Aggregation Propensity of stB wt with Other Stefins. To highlight and provide a rationale for the experimental findings we explored available programs to predict protein aggregation. Figure 5 shows the results of the aggregation predictions for different stefins obtained using Aggrescan.[41] This online server predicts *hot spots*, that is, aggregation-prone regions, in a protein based on their amino acid sequences. The predicted hot spots are shown in red. Predictions obtained for stefins from different organisms differ, and it can be seen that the first aggregation-prone region in human stB includes the stretch MMCGA followed by Pro 6 (shown in bold), which is not part of the hot spot (Figure 5). The same observation holds for mouse and rat stB. Interestingly, human stA, bovine stB, mouse st 2 and 3, bovine stA, and mouse stA do not have hot spots in this region, but note that they do not have Pro at position 6 either (shown in blue). The only exception in this set of proteins is mouse st 1, whose first hot spot includes the first 6 amino acid residues but without a Pro in the vicinity (Figure 5). Moreover, the role of the highly conserved Pro 74 cannot be neglected, because all stefins with Pro 74 have a hot spot in its close vicinity (Figure 5). These observations once more suggest that Pro 6 and Pro 74 contribute strongly to the amyloid propensity of stB wt.

Figure 5. Bioinformatics: AGGRESCAN predictions of hot spots in structures of different stefins. Hot spots are shown in red, Pro residues are bold, and other relevant residues are shown in blue. Amino acid sequences are taken from UniProtKB (2017).

DOI: 10.1021/acschemneuro.8b00621
ACS Chem. Neurosci. 2019, 10, 2730−2740

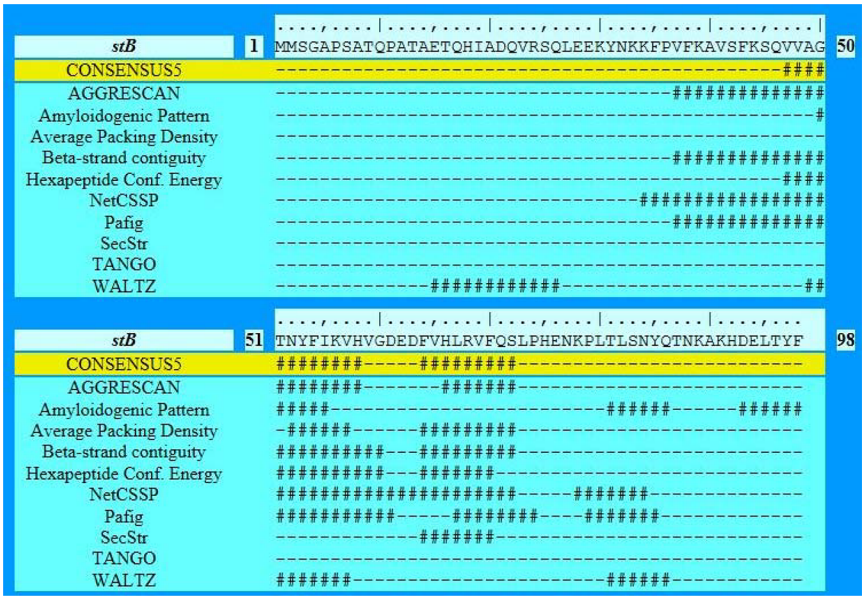

Figure 6. Prediction of aggregation-prone regions within human stB protein. The prediction of aggregation-prone regions within human stB protein was performed using a consensus web tool AMYLPRED2 (Tsolis et al., 2013) as described in the Methods section. A consensus prediction of at least five different algorithms (CONSENSUS5) and the output of 10 different algorithms are indicated in the panel below the protein sequence. The symbol "#" labels the hits.

It is known that proteins avoid aggregation through conservation of certain amino acid residues; aggregation-prone regions are often surrounded by Pro, Lys, Arg, Glu.[42] Pro residues act as β-sheet breakers, and the following four residues display low aggregation propensity due to their charge and low hydrophobicity.[4] Thus, surface exposure and the amino acid stretch preceding/following Pro 6 and Pro 74 strongly suggest their roles as switches, regulating amyloid fibrillation reaction.

2.5. Comparing Aggregation Propensity of stB wt with Its Pro Mutants. To assess the aggregation propensity of stB wt and its Pro mutants we applied a consensus prediction tool AMYLPRED2.[43] Figure 6 shows a representative output for the case of stB wt. A consensus prediction of at least five different algorithms (CONSENSUS5) highlights two main aggregation-prone regions, namely, V^{47}VAGTNYFIKVH^{58} and F^{64}VHLRVFQS^{72}.

A similar analysis performed on the experimentally tested stB Pro mutants (Figure 3 and Figure 4) shows that these hot spots are also conserved in all mutants (Table 2). In addition, two Pro mutants, P36D and P79S, exhibit an additional hot spot, namely, V^{37}FK^{39} and T^{81}LSN^{84}, respectively. The latter hot spot is also present in the double mutant P74S P79S. The special hot spot of P79S predicted by AMYLPRED2 is not reproduced by the experimentally determined rate or morphology of P79S fibrils.

In human cystatin C, which is a member of the cystatin family I25B, three regions with high aggregation propensity were predicted (^{47}LQVVR^{51}, ^{56}IVAGVNYFLD^{65}, and ^{95}AFCSFQIYAVP^{105}) and confirmed to form amyloid fibrils in vitro.[44,45] Interestingly, a sequence alignment of human cystatin C and human stB shows that these three regions exhibit high sequence similarity (they correspond to F^{38}KAVS^{42}, V^{47}VAGTNYFIK^{56}, and L^{82}SNYQTNKAK^{91} in stB), thus suggesting a fundamental contribution of these regions in forming the aggregation-prone core of stB.[45]

Furthermore, the aggregation propensity of stB wt was compared with its Pro mutants using AGGRESCAN3D (Figure 7), because the spatial arrangement of Pro positions may also be important. In contrast to the experimental data, which offered convincing evidence that mutating P6 and P74 strongly inhibits amyloid fibrillation by stB, this effect was not reproduced by AGGRESCAN3D. According to the prediction

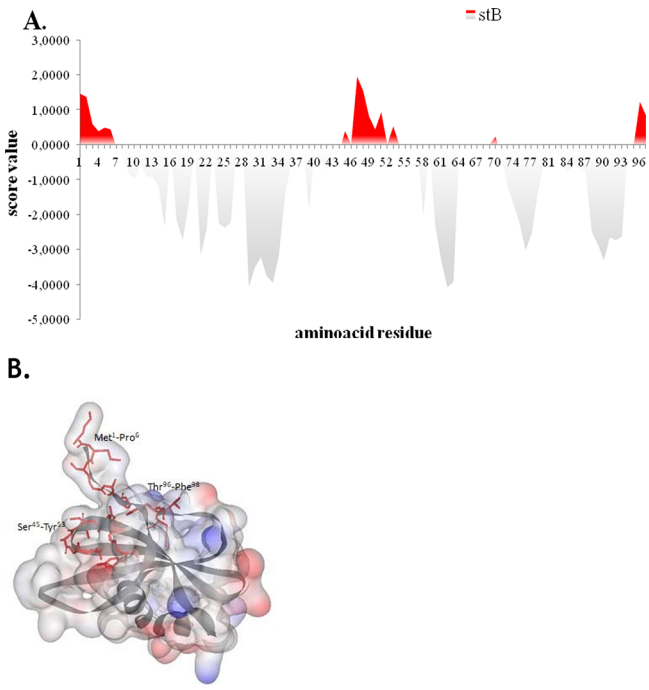

Figure 7. Bioinformatics. (A) Aggregation-prone regions in stB as predicted by AGGRESCAN3D. (B) Three-dimensional structure of stB with predicted hot spots, which include Met^1-Pro^6, Ser45-Tyr53, Thr96-Phe98 (PDB id: 1STF:I). The amino acid residues were labeled as in the protein sequence.

DOI: 10.1021/acschemneuro.8b00621
ACS Chem. Neurosci. 2019, 10, 2730−2740

of AGGRESCAN3D, stB wt and all of its Pro mutants have three hot spots, which include Met 1−Pro 6, Ser 45−Tyr 53, and Thr 96−Phe 98 (Figure 7, stB is shown for reference). Thus, only Pro 6 appears to be part of a hot spot. Experimentally, P6L and all the double mutants thereof indeed show a strong influence on the kinetics of fibrillation (Figure 3). In contrast, P36D shows different behavior without a lag phase (Figure 3), and more aggregates than fibrils are observed at the end of the reaction (Figure 4).

2.6. Results of Kinetic Simulations. To quantify the amyloid fibrillation reaction, we simulated the kinetics using our previous model of amyloid fibril formation by stB,[46] which predicts a nucleation phase where a nucleus of 60 monomers (or 30 dimers) would form. The fitted curves are shown above the ThT fluorescence data in Figure 3A (30 °C) and Figure 3B (37 °C). Each experimental curve was fitted with three parameters (nucleation rate k_I, relative contribution of the prefibrillar phase to the fluorescence signal, and the total amplitude). The growth rate of fibrils (k_G) was assumed as constant for each temperature. Table 3 lists the fitted kinetic constants.

Table 3. Kinetic Parameters, Obtained by Fitting the Fibrillation Kinetics (Figure 3) to the Model Equations[a]

	k_I (s^{-1})	η	k_G (μM^{-1} s^{-1})	k (s^{-1})
protein at 30 °C				
WT	9.04×10^{-6}	0.032	1.3×10^{-3}	
P11S	5.43×10^{-6}	0.27		
P79S	3.58×10^{-6}	0.20		
P36D				6.0×10^{-6}
protein at 37 °C				
WT	2.66×10^{-5}	0.097	6.7×10^{-3}	
P6L	2.35×10^{-5}	0.036		
P11S	1.46×10^{-5}	0.66		
P36D				1.6×10^{-5}

[a] k_I: isomerisation rate, k_G: growth rate, η: amplitude ratio, k: first-order rate constant for downhill polymerization (P36D only).

The mathematical simulations of stB wt and the relevant Pro mutants imply that nucleation is the key process (Table 3 and Figure 3). In accord with the experiments, the critical Pro residues lie either at the N-terminus (P6 and P11) or in the loop region (P74, P79).

In distinction and in accordance to P36G,[23] P36D does not show the lag phase, conforming to downhill polymerization model. Therefore, for this mutant we used a reaction for downhill polymerization (see Methods). It is unclear what causes the observed downhill polymerization of P36D; however, it may be connected to its position as an α-helix breaker (we discussed that in the previous section on stability). Previously, the kinetics without a lag phase was observed for the stB-Y31 variant at pH 3.3 and high salt, where the structured molten globule formed protofibrils as the final stage of the reaction.[28,47] We suggest that P36D (and P36G) could similarly undergo unfolding to a non-native, structured molten globule intermediate with an extended α-helix, which would build protofibrils directly, and the reaction would stop at this stage.

3. CONCLUSIONS

This study confirms that *cis* to *trans* isomerization of critical Pro residues contributes to amyloid fibril formation, starting with domain swapping.[8] Replacement of different Pro residues in human stefin B changes the equilibrium distribution of oligomers at pH 7.5 and substantially influences the kinetics of amyloid fibril formation at pH 4.8. We have shown a crucial role for the *cis* isomer of Pro 74 in the off-pathway tetramer formed by the P79S stB-Y31 variant.[46] Mutation of this residue in P74S stB[17] led to strong inhibition of amyloid formation, which we also observe in this study. Thus, Pro 74 indeed proves to be a key switch toward amyloid fibril formation; the single mutant P74S and all the double and triple mutants containing this substitution exert the largest effects on the inhibition of amyloid fibril formation, both at 30 and 37 °C (Figure 3 and Table 1). Knowing that a *cis* isomer of Pro 74 is present in the tetramer or may already be *cis* in domain-swapped dimers, we thought that another transition from *cis* to *trans* is needed for fibril elongation. In contrast to our expectation that Pro isomerism would affect fibril elongation, the present simulation of the fibrillation kinetics indicates that several Pro residues need to isomerize, separately or in concert, to enable formation of the critical nucleus. In distinction, P36D conforms to a downhill polymerization mechanism without the critical nucleus formation. We argue that a non-native unfolding intermediate forms, leading directly to protofibrils.

4. METHODS

4.1. Preparing Site-Specific Pro Mutants. In this study, we used human stefin B (stB wt) as a model protein. This recombinant protein has Cys 3 replaced by Ser, to avoid disulfide bridge formation in vitro. The starting protein sequence for mutagenesis was a recombinant human stefin B, cloned in 1988,[48] where Y31 was mutated back to E. Mutagenesis was performed by site-directed mutagenesis polymerase chain reaction (PCR) reaction on PCR 2720 Thermal Cycler (Applied Biosystems). Plasmid pET11a was used.

4.2. Expression and Purification. DNA constructs were transformed into the BL21(DE3)pLysS strain of *Escherichia coli*. Expression was induced with isopropyl β-D-1-thiogalactopyranoside (IPTG) (final concentration 1 mM). Cell lysates were additionally purified by adding 4% poly(ethylenimine) (PEI) and centrifuging repeatedly. In this way many contaminants such as nucleic acids and most bacterial, predominantly acidic, proteins were removed from the lysate. The stB wt and all Pro mutants except P74S and P79S were isolated from the purified cell lysate by SEC. Namely, the purified lysate was directly applied to Sephacryl S-100 column (GE Healthcare Life Sciences), which had previously been equilibrated with 0.01 M phosphate buffer, pH 7.8, 0.12 M NaCl. In the next purification step, 2−4 mL of protein sample of 2.5 mg/mL concentration was applied on Superdex 200, which had previously been equilibrated with 0.01 M phosphate buffer, pH 7.5, 0.12 M NaCl. Buffers used for column equilibration were in both cases used for protein elution.

Pro mutants P74S and P79S were purified by affinity chromatography on carboxymethylated (CM) papain-Sepharose (GE Healthcare Life Sciences). The nonspecifically bound material was eluted with 0.01 M Tris-HCl, pH 8.0, 0.5 M NaCl at room temperature. The protein was eluted with 0.02 M triethilamine (TEA) buffer, pH 10.65, and pH was immediately decreased by phosphate-buffered solution (PBS). Additional purification was done using cation-exchange chromatography on SP-Sepharose fast flow (GE Healthcare Life Sciences) in a 0.1 M phosphate buffer at pH 6.05. Recombinant proteins were eluted with a linear gradient of NaCl from 0 to 1 M, in the same buffer. To lower ionic strength, the final protein solution was diluted with the same phosphate buffer without NaCl. After elution from the column, pure folded proteins were obtained.

DOI: 10.1021/acschemneuro.8b00621
ACS Chem. Neurosci. 2019, 10, 2730−2740

4.3. Determination of Protein Concentration. The A_{280} value was determined by Nanodrop (Thermo Fisher Scientific). The specific extinction coefficient and relative molecular mass (M_r) used in the calculations (Supporting Information: Table S1) were determined from the amino acid sequence using Expasy ProtParam tool.[49]

4.4. Determination of Purity of the Recombinant Proteins. To determine the purity of isolated recombinant proteins tricine-SDS-PAGE was used.[25] This is the preferred electrophoretic system for the resolution of proteins smaller than 30 kDa. In each case, 40 μg of each protein was loaded on the gel.

4.5. Determination of Inhibitory Activity against Papain. Papain activity was determined using fluorogenic substrate Z-Phe-Arg-AMC (Bachem) in 96-well plates (Safire, Tecan). Protein samples were incubated in 0.1 M phosphate buffer, pH 6.0, 1.5 mM ethylenediaminetetraacetic acid (EDTA). After 10 min of incubation papain was added, which was previously activated in 0.1 M phosphate buffer, pH 6.0, 1.5 mM EDTA. After another 10 min Z-Phe-Arg-AMC was added, and the fluorescence was measured at 2 min intervals. The final concentration of both papain and protein was 5−10 nM and Z-Phe-Arg 30 μM. A blind probe without papain and protein was followed, and stB wt used as a positive control. The assay was done in triplicates for each protein.

4.6. Circular Dichroism (CD). Far-UV CD spectra were measured at room temperature by using a Circular Dichroism Spectrometer MOS-500 (Bio-Logic Science Instruments). Temperature was maintained at 25 °C throughout. A 1 mm quartz cuvette was used for all CD spectra. Data were recorded from 250 to 200 nm with 1 nm sampling interval. Protein concentrations were such that the final A_{280} was 0.15 (34 μM). The final spectra were the average of three repeated experiments, and the background (the CD spectrum of the buffer without stB wt) was subtracted.

4.7. Analytical Size Exclusion Chromatography (SEC on FPLC). SEC was performed using Superdex 75 column (10 × 300 mm) (Amersham Biosciences), connected to FPLC (Amersham Biosciences) at room temperature. The flow rate was 0.5 mL/min. Protein (500 μL, ∼1 mg/mL) was applied to the column. Phosphate buffer, 10 mM, pH 7.0, 150 mM NaCl was used as standard buffer for column equilibration and elution. The oligomeric state of stB wt was additionally evaluated with cross-linking with BS^3 and SDS-PAGE electrophoresis.

4.8. Kinetics of Amyloid Fibrillation Reaction. ThT dye was used to determine the presence of amyloid-like fibrils. Fluorescence was measured using a PerkinElmer model LS 50 B fluorimeter. For ThT emission, excitation was at 440 nm, and spectra were recorded from 455 to 600 nm. Intensity at 480 nm was plotted against time. ThT dye was dissolved in 25 mM phosphate buffer, pH 7.5, 0.1 M NaCl at 15 μM (A_{416} = 0.66). Fibrils were grown under mild conditions at pH 4.8 (0.015 M acetate buffer, pH 4.8, 0.15 M NaCl at) at 30 °C (Thermomixer comfort, Eppendorf) and 37 °C (WTC, Binder); protein concentrations were 34 μM. To accelerate fibril formation, fibrillation mixtures contained 10% (v/v) TFE, which was shown before to accelerate fibril formation of stefin B at this particular concentration.[28,50] At higher concentrations this organic solvent causes transition of proteins to an all α-helical state.[51] To initiate amyloid fibrils' formation the transition to a partially folded intermediate with more β-structure must take place; therefore, we took the appropriate concentration of TFE.[50] To measure the contents of the ThT binding fibrils, 50 μL of the protein solution was added to 570 μL of the ThT buffer just before the measurement. Fresh ThT probe was prepared daily.

4.9. Transmission Electron Microscopy (TEM). Protein samples (15 μL of 34 μM protein solution) were applied on a Formvar and carbon-coated grid. After 3 min the sample was soaked away and stained with 1% (w/v) uranyl acetate. Samples were observed with a Philips CM 100 (FEI) transmission electron microscope operating at 80 kV. Images were recorded by Bioscan CCD or ORIUS SC 200 camera (Gatan Inc.), using Digital Micrograph software (Gatan Inc.). Two parallel grids were prepared for each sample, at least 10 grid squares were inspected thoroughly, and many micrographs were taken of each grid.

4.10. Bioinformatics and Simulations. To compare aggregation propensity of stB wt with other stefins, their aggregation profiles were determined using AGGRESCAN.[52] This server assumes protein behavior based on an aggregation propensity scale of amino acid residues arising from the in vivo studies. Amino acid sequences were taken from UniProtKB.[53]

The prediction of amyloid-prone regions within human stB protein and its proline mutants was performed using a web tool AMYLPRED2[43] accessible at http://aias.biol.uoa.gr/AMYLPRED2. It is a sequence-based approach that uses a consensus of different methods (Aggrescan, AmyloidMutants, Amyloidogenic Pattern, Average Packing Density, Beta-strand contiguity, Hexapeptide Conformational Energy, NetCSSP, Pafig, SecStr, Tango, and Waltz) that have been specifically developed to predict features related to the formation of amyloid fibrils. The consensus of these methods is the primary output of the program, and it is defined as the hit overlap of at least $n/2$ (rounded down) of n selected methods (i.e., 5 of 11 methods, if the user chooses to use all available methods). However, the individual predictions of these methods are also available.

Furthermore, we used AGGRESCAN3D (A3D).[54] This server takes into account the protein structure and the experimental aggregation propensity scale from the well-established AGGRESCAN method. With the A3D server, certain residues can be virtually mutated to design different variants, which made it a perfect candidate for studying effects of Pro mutations on aggregation propensity of stB wt.

The mathematical simulation of the nucleation and growth kinetics followed the scheme as described in our previous work by Škerget et al., 2009.[46]

Because of the lower protein concentration (and because we do not study the concentration dependence), we reduced the model by excluding the off-pathway state and the residual concentration, that is, by setting the constants K_0, k_{-OP}, and c_R to 0. We solved the system of differential equations with the Runge−Kutta method (routine D02PCF from the NAG library, Numerical Algorithms Group). The parameters were fitted with a nonlinear least-square method (NAG routine E04FYF). To fit the different kinetics of P36D, which does not show any lag phase, the equation for downhill polymerization was used with n = 1, which reduces it to a first-order rate equation, resulting in an exponential dependence of the intensity $I(t) = A(1 - \exp(-kt))$.

■ ASSOCIATED CONTENT

Supporting Information

The Supporting Information is available free of charge on the ACS Publications website at DOI: 10.1021/acschemneuro.8b00621.

Molecular parameters obtained by Expasy ProtParam, purity of the recombinant proteins, inhibitory activity against papain, CD spectra, analytical SEC data, and thermal stability (PDF)

Accession Codes

Human stefin B (stB) - UniProtKB - P04080 (CYTB_HUMAN)

■ AUTHOR INFORMATION

Corresponding Author

*E-mail: eva.zerovnik@ijs.si. Phone ++386 1 477 3753.

ORCID

Andrej Vilfan: 0000-0001-8985-6072

Eva Žerovnik: 0000-0002-9793-8200

Author Contributions

E.Ž. and S.H. designed and performed experiments. Initial experiments were done by A.T.-V.; S.H. wrote the paper draft, and E.Ž. finalized the paper. M.T.Ž. measured and analyzed

DOI: 10.1021/acschemneuro.8b00621
ACS Chem. Neurosci. 2019, 10, 2730−2740

TEM, A.V. performed kinetic simulations, and V.S. contributed with bioinformatics. All, including S.B. and V.P., added to Discussion. E.Ž. is the responsible and corresponding author.

Funding

This work was supported by the Slovenian Research Agency (ARRS) program P1-0140 "Proteolysis and its regulation" led by B. Turk, Ljubljana, Slovenia. S.H. was given a Fellowship via CMEPIUS for studying at the Jožef Stefan International Postgraduate School (Ljubljana, Slovenia).

Notes

The authors declare no competing financial interest.

■ ACKNOWLEDGMENTS

Authors thank Mr. J. Novak from Nanotemper for giving us opportunity to measure protein stability by NanoDSF assay during demonstration. We thank Prof. J. Waltho (Univ. Sheffield and Univ. Manchester, UK) to read and comment the final version of the paper and Prof. V. Turk (IJS, Ljubljana, Slovenia) to discuss certain isuues related to stefins structure and function.

■ ABBREVIATIONS:

(CD), circular dischroism; TEM, transmission electron microscopy; (ThT), Thioflavin T

■ REFERENCES

(1) Knowles, T. P. J., Vendruscolo, M., and Dobson, C. M. (2014) The amyloid state and its association with protein misfolding diseases. *Nat. Rev. Mol. Cell Biol. 15*, 384.

(2) Scheckel, C., and Aguzzi, A. (2018) Prions, prionoids and protein misfolding disorders. *Nat. Rev. Genet. 19*, 405.

(3) Lee, C. C., Nayak, A., Sethuraman, A., Belfort, G., and McRae, G. J. (2007) A three-stage kinetic model of amyloid fibrillation. *Biophys. J. 92*, 3448−3458.

(4) Monsellier, E., and Chiti, F. (2007) Prevention of amyloid-like aggregation as a driving force of protein evolution. *EMBO Rep. 8*, 737−742.

(5) Berry, A. (2001) Protein folding and its links with human disease. *Biochem. Soc. Symp. 68*, 1−26.

(6) Radwan, M., Wood, R. J., Sui, X., and Hatters, D. M. (2017) When proteostasis goes bad: Protein aggregation in the cell. *IUBMB Life 69*, 49−54.

(7) MacArthur, M. W., and Thornton, J. M. (1991) Influence of proline residues on protein conformation. *J. Mol. Biol. 218*, 397−412.

(8) Taler-Vercic, A. (2017) Proline Residues as Switches in Conformational Changes Leading to Amyloid Fibril Formation. *Int. J. Mol. Sci. 18*, 549 DOI: 10.3390/ijms18030549.

(9) Ryo, A., et al. (2006) Prolyl-isomerase Pin1 accumulates in lewy bodies of parkinson disease and facilitates formation of alpha-synuclein inclusions. *J. Biol. Chem. 281*, 4117−4125.

(10) Kumar, T. K. S., Samuel, D., Jayaraman, G., Srimathi, T., and Yu, C. (1998) The role of proline in the prevention of aggregation during protein folding in vitro. *Biochem. Mol. Biol. Int. 46*, 509−517.

(11) Rauscher, S., Baud, S., Miao, M., Keeley, F. W., and Pomès, R. (2006) Proline and Glycine Control Protein Self-Organization into Elastomeric or Amyloid Fibrils. *Structure 14*, 1667−1676.

(12) Rousseau, F., Schymkowitz, J. W., Wilkinson, H. R., and Itzhaki, L. S. (2001) Three-dimensional domain swapping in p13suc1 occurs in the unfolded state and is controlled by conserved proline residues. *Proc. Natl. Acad. Sci. U. S. A. 98*, 5596−5601.

(13) Rousseau, F., Schymkowitz, J. W. H., and Itzhaki, L. S. (2003) The unfolding story of three-dimensional domain swapping. *Structure 11*, 243−251.

(14) Salahuddin, A. (1984) Proline Peptide Isomerization and Protein Folding. *J. Biosci. 6*, 349−355.

(15) Shaw, P. E. (2002) Peptidyl-prolyl isomerases: a new twist to transcription. *EMBO Rep. 3*, 521−526.

(16) Brandts, J. F., Halvorson, H. R., and Brennan, M. (1975) Consideration of the Possibility that the slow step in protein denaturation reactions is due to cis-trans isomerism of proline residues. *Biochemistry 14*, 4953−4963.

(17) Smajlovic, A., et al. (2009) Essential role of Pro 74 in stefin B amyloid-fibril formation: dual action of cyclophilin A on the process. *FEBS Lett. 583*, 1114−1120.

(18) Turk, V., et al. (2012) Cysteine cathepsins: From structure, function and regulation to new frontiers. *Biochim. Biophys. Acta, Proteins Proteomics 1824*, 68−88.

(19) Turk, V., Stoka, V., and Turk, D. (2008) Cystatins: biochemical and structural properties, and medical relevance. *Front Biosci 13*, 5406−5420.

(20) Turk, B., Colic, A., Stoka, V., and Turk, V. (1994) Kinetics of Inhibition of Bovine Cathepsin-S by Bovine Stefin-B. *FEBS Lett. 339*, 155−159.

(21) Stoka, V., et al. (1995) Inhibition of Cruzipain, the Major Cysteine Proteinase of the Protozoan Parasite, Trypanosoma-Cruzi, by Proteinase-Inhibitors of the Cystatin Superfamily. *FEBS Lett. 370*, 101−104.

(22) Stubbs, M. T., et al. (1990) The refined 2.4 A X-ray crystal structure of recombinant human stefin B in complex with the cysteine proteinase papain: a novel type of proteinase inhibitor interaction. *EMBO J. 9*, 1939−1947.

(23) Kenig, M., et al. (2004) Differences in aggregation properties of three site-specific mutants of recombinant human stefin B. *Protein Sci. 13*, 63−70.

(24) Kenig, M., et al. (2006) Folding and amyloid-fibril formation for a series of human stefins' chimeras: any correlation? *Proteins: Struct., Funct., Genet. 62*, 918−927.

(25) Taler-Vercic, A., et al. (2013) The role of initial oligomers in amyloid fibril formation by human stefin B. *Int. J. Mol. Sci. 14*, 18362−18384.

(26) Anderluh, G., and Zerovnik, E. (2012) Pore formation by human stefin B in its native and oligomeric states and the consequent amyloid induced toxicity. *Front. Mol. Neurosci. 5*, 85.

(27) Zerovnik, E., et al. (2007) Amyloid fibril formation by human stefin B: influence of pH and TFE on fibril growth and morphology. *Amyloid 14*, 237−247.

(28) Zerovnik, E., et al. (2002) Human stefin B readily forms amyloid fibrils in vitro. *Biochim. Biophys. Acta, Protein Struct. Mol. Enzymol. 1594*, 1−5.

(29) Zerovnik, E., Jerala, R., Kroon-Zitko, L., Pain, R. H., and Turk, V. (1992) Intermediates in denaturation of a small globular protein, recombinant human stefin B. *J. Biol. Chem. 267*, 9041−9046.

(30) Zerovnik, E., Jerala, R., Kroon-Zitko, L., Turk, V., and Pain, R. H. (1992) Denaturation of stefin B by GuHCl, pH and heat; evidence for molten globule intermediates. *Biol. Chem. Hoppe-Seyler 373*, 453−458.

(31) Zerovnik, E., Virden, R., Jerala, R., Turk, V., and Waltho, J. P. (1998) On the mechanism of human stefin B folding: I. Comparison to homologous stefin A. Influence of pH and trifluoroethanol on the fast and slow folding phases. *Proteins: Struct., Funct., Genet. 32*, 296−303.

(32) Zerovnik, E., et al. (1998) On the mechanism of human stefin B folding: II. Folding from GuHCl unfolded, TFE denatured, acid denatured, and acid intermediate states. *Proteins: Struct., Funct., Genet. 32*, 304−313.

(33) Jenko Kokalj, S., et al. (2007) Essential role of proline isomerization in stefin B tetramer formation. *J. Mol. Biol. 366*, 1569−1579.

(34) Morgan, G. J., et al. (2008) Exclusion of the native alpha-helix from the amyloid fibrils of a mixed alpha/beta protein. *J. Mol. Biol. 375*, 487−498.

(35) Ceru, S., and Zerovnik, E. (2008) Similar toxicity of the oligomeric molten globule state and the prefibrillar oligomers. *FEBS Lett. 582*, 203−209.

DOI: 10.1021/acschemneuro.8b00621
ACS Chem. Neurosci. 2019, 10, 2730−2740

(36) Eakin, C. M., Attenello, F. J., Morgan, C. J., and Miranker, A. D. (2004) Oligomeric assembly of native-like precursors precedes amyloid formation by beta-2 microglobulin. *Biochemistry 43*, 7808−7815.
(37) Greenfield, N. J. (2006) Using circular dichroism spectra to estimate protein secondary structure. *Nat. Protoc. 1*, 2876−2890.
(38) Staniforth, R. A., et al. (2001) Three-dimensional domain swapping in the folded and molten-globule states of cystatins, an amyloid-forming structural superfamily. *EMBO J. 20*, 4774−4781.
(39) LeVine, H., 3rd (1999) Quantification of beta-sheet amyloid fibril structures with thioflavin T. *Methods Enzymol. 309*, 274−284.
(40) Newby, G. A., et al. (2017) A Genetic Tool to Track Protein Aggregates and Control Prion Inheritance. *Cell 171*, 966−979 e918 .
(41) Conchillo-Sole, O., et al. (2007) AGGRESCAN: a server for the prediction and evaluation of "hot spots" of aggregation in polypeptides. *BMC Bioinf. 8*, 65.
(42) Rousseau, F., Schymkowitz, J., and Serrano, L. (2006) Protein aggregation and amyloidosis: confusion of the kinds? *Curr. Opin. Struct. Biol. 16*, 118−126.
(43) Tsolis, A. C., Papandreou, N. C., Iconomidou, V. A., and Hamodrakas, S. J. (2013) A Consensus Method for the Prediction of "Aggregation-Prone" Peptides in Globular Proteins. *PLoS One 8*, e54175.
(44) Tsiolaki, P. L., Hamodrakas, S. J., and Iconomidou, V. A. (2015) The pentapeptide LQVVR plays a pivotal role in human cystatin C fibrillization. *FEBS Lett. 589*, 159−164.
(45) Tsiolaki, P. L., Louros, N. N., Hamodrakas, S. J., and Iconomidou, V. A. (2015) Exploring the "aggregation-prone" core of human Cystatin C: A structural study. *J. Struct. Biol. 191*, 272−280.
(46) Skerget, K., et al. (2009) The mechanism of amyloid-fibril formation by stefin B: temperature and protein concentration dependence of the rates. *Proteins: Struct., Funct., Genet. 74*, 425−436.
(47) Zerovnik, E., Turk, V., and Waltho, J. P. (2002) Amyloid fibril formation by human stefin B: influence of the initial pH-induced intermediate state. *Biochem. Soc. Trans. 30*, 543−547.
(48) Jerala, R., Trstenjak, M., Lenarcic, B., and Turk, V. (1988) Cloning a synthetic gene for human stefin B and its expression in E. coli. *FEBS Lett. 239*, 41−44.
(49) Wilkins, M. R., et al. (1998) Protein identification and analysis tools in the ExPASy server. *Methods Mol. Biol. 112*, 531−552.
(50) Zerovnik, E., et al. (1999) Differences in the effects of TFE on the folding pathways of human stefins A and B. *Proteins: Struct., Funct., Genet. 36*, 205−216.
(51) Shiraki, K., Nishikawa, K., and Goto, Y. (1995) Trifluoroethanol-Induced Stabilization of the Alpha-Helical Structure of Beta-Lactoglobulin - Implication for Non-Hierarchical Protein-Folding. *J. Mol. Biol. 245*, 180−194.
(52) de Groot, N. S., Castillo, V., Grana-Montes, R., and Ventura, S. (2012) AGGRESCAN: method, application, and perspectives for drug design. *Methods Mol. Biol. 819*, 199−220.
(53) Boutet, E., et al. (2016) UniProtKB/Swiss-Prot, the Manually Annotated Section of the UniProt KnowledgeBase: How to Use the Entry View. *Methods Mol. Biol. 1374*, 23−54.
(54) Zambrano, R., et al. (2015) AGGRESCAN3D (A3D): server for prediction of aggregation properties of protein structures. *Nucleic Acids Res. 43*, W306−313.

DOI: 10.1021/acschemneuro.8b00621
ACS Chem. Neurosci. 2019, 10, 2730−2740